Eur. Phys. J. A **29**, 53–57 (2006)
DOI 10.1140/epja/i2005-10298-4

THE EUROPEAN PHYSICAL JOURNAL A

Numerical studies of QGP instabilities and implications

G.D. Moore[a]

Department of Physics, McGill University, 3600 rue University, Montréal QC H3A 2T8, Canada

Received: 16 November 2005 /
Published online: 6 September 2006 –

Abstract. Because of the flat initial shape of the QGP in a heavy-ion collision, the momentum distribution becomes anisotropic after a short time. This leads to plasma instabilities, which may help explain how the plasma isotropizes. We explain the physics of instabilities and give the latest results of numerical simulations into their evolution. Non-Abelian interactions cut off the size to which the soft unstable fields grow, and energy in the soft fields subsequently cascades towards more ultraviolet scales. We present first results for the power spectrum of this cascade.

PACS. 12.38.Mh Quark-gluon plasma – 11.10.Wx Finite-temperature field theory – 11.15.Ha Lattice gauge theory

1 Introduction

When relativistic nuclei collide, they leave behind a plasma of quarks and (mostly) gluons which starts out in a flat pancake-shaped region of space. This simply reflects the fact that the nuclei are approximately spherical in their rest frames, but the Lorentz boost of their motion compresses them along the beam axis into nearly flat sheets. Further, if the collision is not perfectly head-on but occurs at a finite impact parameter (as is usually the case), the initial region is not circular in the transverse plane, either; it looks instead like a "flat almond," as depicted in fig. 1.

This flat initial shape will quickly change, as the region containing quark-gluon plasma expands into the space around it. If the quarks and gluons stream freely (as they would, at least initially, if the coupling α_s were truly small), then "momentum selection" will make the plasma locally highly anisotropic, see fig. 2.

In the absence of rescattering, the momentum distribution reaching detectors would be isotropic, since the initial distribution of particles was. If rescattering is efficient, then the momentum distribution relaxes to be isotropic, *locally* at each point, and with respect to the local rest frame, which is a moving frame with respect to the system as a whole. For instance, in the right-hand picture in fig. 2, the particles on the right side of the almond would redistribute to be isotropic with respect to their (rightward moving) local rest frame. Because the initial shape is anisotropic, there are more left- and right-moving "cells" of plasma than up- and down-moving "cells". The $p_\perp^2$ summed over particles gets one contribution from the $p_\perp^2$ of the particle relative to its cell, and one from the $p_\perp^2$ of the cell. The first is equal between p_x^2 and p_y^2 if rescattering isotropizes locally. The second favors the direction which was initially the skinny direction of the almond. Therefore, the momentum distribution of final particles will favor the initially thin axis of the almond, *if* rescattering occurs. This is called elliptic flow, and it is observed to be nearly maximal in heavy-ion collisions [1,2], that is, nearly at the value obtained if rescattering is perfectly efficient.

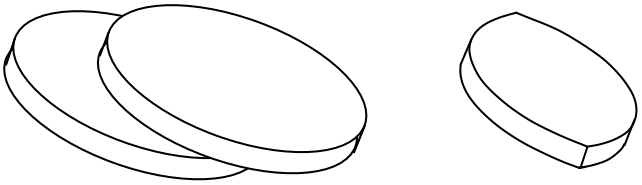

Fig. 1. Left: pancake-shaped nuclei just before colliding. Right: resulting "flat-almond"–shaped region of quark-gluon plasma.

It has been argued [3] that the elliptic flow observed in heavy-ion collisions is incompatible with the plasma being weakly coupled. That is, perturbative treatments of the QGP [4] seem to be at a loss to explain how it can show as much elliptic flow as it seems to[1]. However, before discarding the idea of weak coupling, we should first make sure that the weak-coupling treatments were done correctly. We argue that weak-coupling treatments

[a] e-mail: guymoore@physics.mcgill.ca

[1] Inclusion of number changing processes may change this conclusion [5]. This is an interesting development, though we are concerned that those treatments do not include virtual (suppressing) corrections to the $2 \leftrightarrow 2$ cross-section.

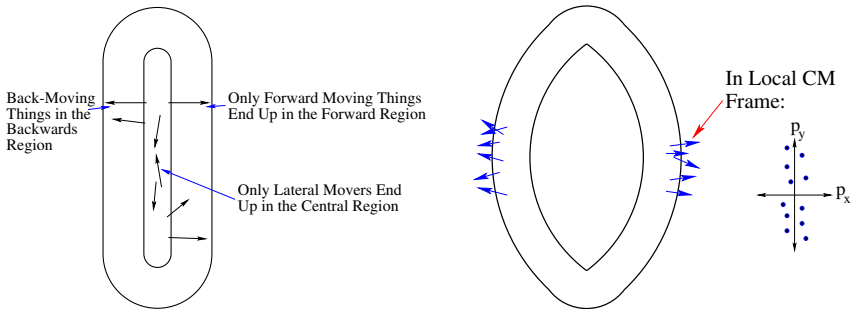

Fig. 2. Left: momentum selection along the beam axis: forward-moving particles end up in front, backwards movers in back, and only lateral movers remain in the middle. Right: the same applies in the transverse plane.

to date leave out the dominant physics, which has to be understood before such strong claims can be made with confidence.

2 Plasma instabilities

Consider first what the traditional treatment of scattering in a plasma is. The particles in the plasma are considered to undergo $2 \leftrightarrow 2$ scattering. The scattering rate has a (Coulombic) soft divergence, $\mathrm{d}\sigma \sim \mathrm{d}^2 q_\perp / q_\perp^4$. To find out how much this isotropizes the plasma one must multiply by q^2 to get the transport cross-section, but this is still log divergent:

$$\sigma_{\mathrm{transport}} \propto g^4 \int q^2 \mathrm{d}q^2 \frac{1}{q^4} \,. \tag{1}$$

This means that it is essential to include plasma corrections to the scattering. In equilibrium, this leads to a finite result [6]:

$$\begin{aligned} \sigma_{\mathrm{transport}} &\propto g^4 \int q^2 \mathrm{d}q^2 \frac{1}{(q^2+\Pi)^2} \\ &\sim g^4 \int q_\perp^2 \mathrm{d}q_\perp^2 \frac{1}{q_\perp^2 (q_\perp^2 + m_{\mathrm{D}}^2)} \,. \end{aligned} \tag{2}$$

(Here Π represents the self-energy and m_{D}^2 is the Debye mass squared.) Plasma effects cut off the small-angle scattering rate. However, Π was derived using the *isotropic* equilibrium result for the self-energy. For a nonequilibrium plasma, one should recompute the self-energy for the nonequilibrium, *anisotropic* particle distribution. The relevant self-energies are known [7], but when they are inserted in the scattering calculation, they lead to propagators which are singular at finite momentum and give an apparently divergent answer for $\sigma_{\mathrm{transport}}$ [8].

We should examine the self-energy more carefully. The leading "hard loop" [9,10] self-energy represents the current induced by the coherent response of the plasma to an infrared gauge field. The simplest example to think about is a plasma oscillation, which we will now describe for an Abelian (E&M) plasma. Suppose that there is a spatially uniform **E** field in the plasma. Each + charge will be deflected into the direction of the **E** field, each − charge will be deflected against it. For a + and − charge at the same location and direction, the + moves in the **E**-direction and the − against that direction, leading to a small dipole. Each individual deflection is small, but there are a lot of particles and the deflections build up over time. The individual dipoles add up into an **E** field opposing the original one, which soon cancels off the initial **E** field completely. But the particles keep following the deflected trajectories, so the dipoles continue to grow, and the total **E** field reverses sign. Then the particles deflect back the other way, leading back to the starting configuration. The **E** field will oscillate back and forth in sign at a characteristic frequency ω_{pl} determined by the density and deflectability of the charges in the plasma.

Now, consider a more complex and relevant example, shown in fig. 3. Suppose an anisotropic plasma has all charges flow along one "beam" direction. Consider a seed magnetic field with **k** and **B** orthogonal to the beam. The particles deflect in the magnetic field; the + charges are focused where the − charges are defocused, leading to a net current. The current is exactly the one which supports the magnetic field which started the trouble. Since the deflection grows with time, the current will become large enough to generate and even strengthen **B**. This will lead to greater charge deflection, greater current, and greater **B**. This is an exponential instability, called the *Weibel instability*, known in the plasma physics community since the 1950s [11]. Though we discussed the case of maximal instability, the same process is present whenever the plasma is anisotropic. The time scale for this instability to grow is short: if typical momenta are $\mathrm{O}(T)$ and the particle density is $\mathrm{O}(T^3)$, but the momentum distribution is anisotropic, the growth rate of the instability is $\gamma \sim gT$, to be compared with the large angle particle scattering rate (in equilibrium) of $\Gamma \sim g^4 T$. Therefore the **B** fields become large on a scale shorter than any scattering time scale in the plasma. In fact, it is generally faster than *any* dynamical time scale in the plasma, or the system age [12], and *must* be considered in understanding the evolution of the plasma.

3 Kinetic theory treatment

We would like to address plasma instabilities in the context of the full QGP evolution at realistic coupling. That

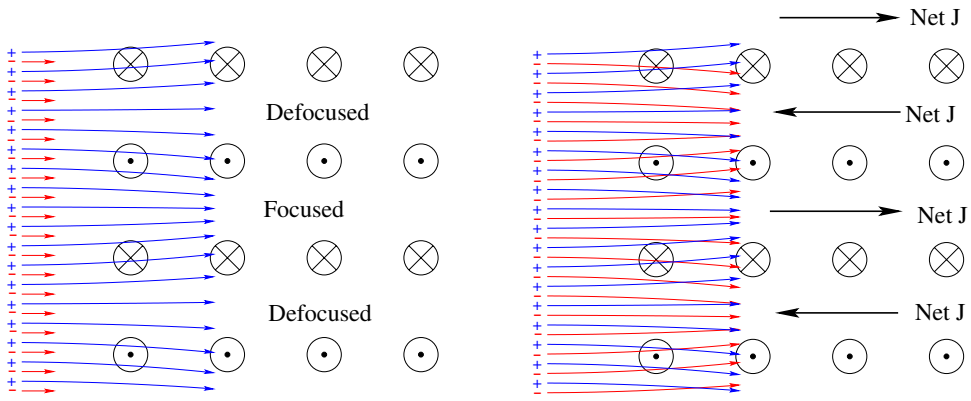

Fig. 3. Left: magnetic field and particle distribution which is unstable, and the deflection of + charges. Right: deflection of all charges, and induced currents. The current is exactly the one which supports the magnetic field.

is a big task. We take instead the warmup task of understanding the behavior in the limit of weak coupling $\alpha_{\rm s} \ll 1$, some time after the collision when the plasma has become anisotropic, and working only in a local patch of plasma which is statistically spatially uniform. The key is that the particle density n becomes smaller than the nonperturbative size, $n \ll p^3/\alpha_{\rm s}$, with p the typical momentum of a hard particle. Therefore the screening scale $m^2 \sim \alpha n/p$ becomes $m \ll p$; there is a separation of scale between the wave number of the unstable modes and of the dominant excitations in the plasma. This allows a separation of the degrees of freedom. The soft modes will achieve large occupancy due to the instability, and may therefore be treated as classical fields. The dominant modes have large momentum and may therefore be treated as particles. This allows a Vlasov equation treatment.

In equilibrium, an electric field polarizes the plasma, but a magnetic field merely rotates the isotropic distribution of momenta, which does not induce a net current. For an anisotropic plasma, though, the distribution of particles,

$$\Omega(\mathbf{v}) \equiv \frac{1}{\int \mathrm{d}^3p f(p)/p} \int \frac{\mathrm{d}^3\mathbf{p}}{p} f(\mathbf{p}) \delta(\hat{\mathbf{p}} - \mathbf{v}) \qquad (3)$$

is not isotropic. ($\Omega(\mathbf{v})$ represents the number of particles moving in the $\mathbf{v}$-direction, weighted by their "bendability" $1/p$ and normalized to average to 1 over angles.) This means that any electromagnetic field can induce a current. In particular, defining the net color of particles moving in the $\mathbf{v}$-direction at point $\mathbf{x}$ as $W^a(\mathbf{x},\mathbf{v})$, the joint equations for W and A_μ are

$$D_t W^a(x,\mathbf{v}) = -\mathbf{v}\cdot\mathbf{D}W^a(x,\mathbf{v}) + m_\infty^2 \text{ Source}\,, \qquad (4)$$

$$\text{Source} = 2\Omega(\mathbf{v})\mathbf{v}\cdot\mathbf{E}^a - \mathbf{E}^a\cdot\frac{\partial}{\partial\mathbf{v}}\Omega(\mathbf{v}) - F^a_{ij}v_i\frac{\partial\Omega(\mathbf{v})}{\partial v_j}\,, \qquad (5)$$

$$D_\mu F^{\nu\mu} = J^\nu = \int_{\mathbf{v}} v^\nu\, W(\mathbf{v}). \qquad (6)$$

The first equation describes the (covariant) free propagation of particles, $v^\mu D_\mu W = 0$, modified by the induced current from polarizing the mean (colorless) distribution of particles. The parameter $m_\infty^2 = g^2 C_f \int \mathrm{d}^3p f(p)/p$ equals $m_{\rm D}^2/2$ in equilibrium and gives the polarizability of the medium. The second line shows how much $\mathbf{E}$ and $\mathbf{B}$ fields polarize the medium. The last line is the Yang-Mills equation with J determined by W.

These equations can be solved two ways. They can be handled analytically in the context of weak-field perturbation theory. This has been pursued quite far [13,12]. The conclusion is that any anisotropy causes exponential growth, and O(1) anisotropy (Ω deviating by O(1) amounts from being isotropic) leads to an exponentiation time $\gamma \sim m_\infty$. At any time later than the formation time of the plasma, multiple exponentiation times have occurred, and one must deal with the fully nonlinear equations. These are not tractable analytically, and we must use the other technique for solving these equations: numerical implementation.

The classical Yang-Mills equations can be solved nonperturbatively in real (Minkowski) time on the lattice via existing techniques [14]. The W fields have been added to such a lattice simulation for an isotropic plasma in [15]. New difficulties emerge in this treatment, because W^a is a function of $\mathbf{v}$ as well as $\mathbf{x}$; both must be discretized somehow to make the system finite. Reference [15] does so by expanding functions of $\mathbf{v}$ in spherical harmonics and truncating at a finite $\ell_{\rm max}$. It is also possible to discretize the sphere directly [16]. Here we will present results using the $\ell_{\rm max}$ cutoff technique, extended to anisotropic Ω [17]. We work in $SU(2)$ rather than $SU(3)$ for simplicity; we expect the qualitative behavior to be the same, and the simulations remain at the level of understanding the gross features rather than the quantitative details at this time.

4 Numerical results

We summarize results obtained jointly with Peter Arnold and Larry Yaffe, which have recently been presented in greater detail [17,18].

If the gauge fields are initially small, they grow exponentially, as expected perturbatively, until they are nonperturbatively large. At this point, the growth in the gauge field energy changes over to linear behavior, see

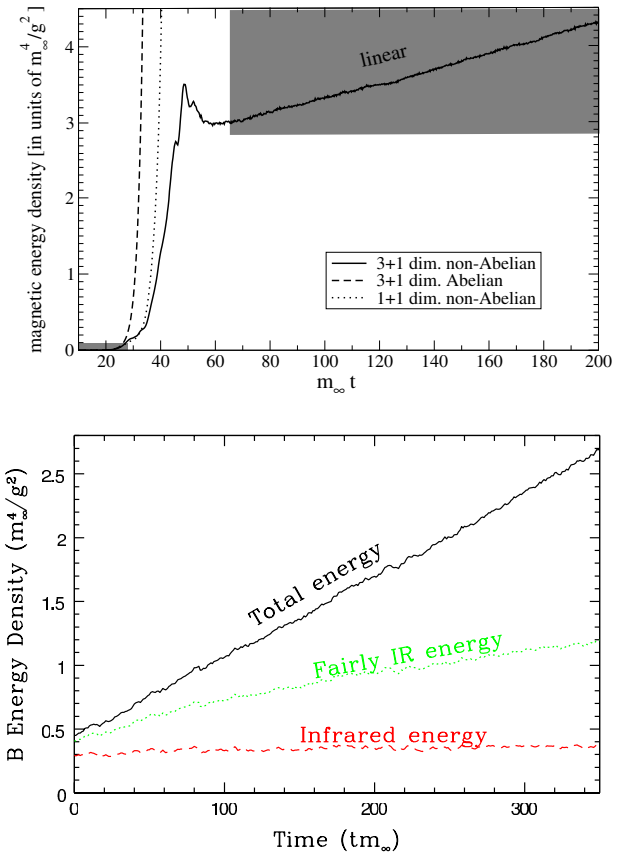

Fig. 4. Top: energy growth from small seed fields is exponential at first but becomes linear when the fields become nonperturbative. Bottom: for nonperturbative seeds, the growth is always linear; but the energy gain is in the higher **k** modes only, as revealed by smearing.

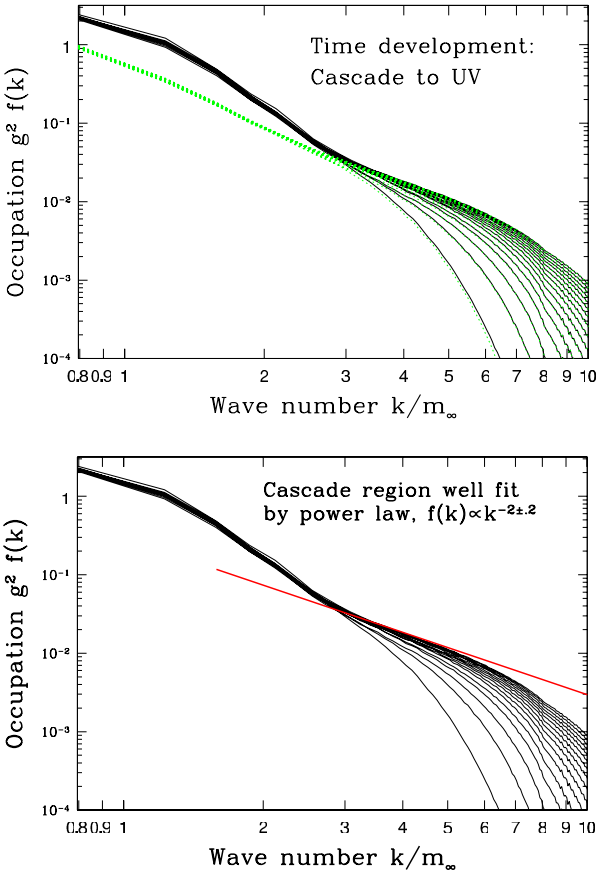

Fig. 5. Top: Coulomb gauge spectrum from E (lower at left) and A (higher at left) fields, at a series of times from early (bottom at right) to late (top at right). Bottom: the same, with a suggestive power law fit superimposed. It appears that $f(k) \propto k^{-2}$.

fig. 4. What does this behavior represent? By "smearing" the fields to remove high-**k** components, we can demonstrate (same figure) that the infrared fields do *not* grow any more, but the energy goes into ever more ultraviolet degrees of freedom.

This behavior is confirmed by looking at the power spectrum of the electric and magnetic energy in Coulomb gauge. In a system of quasiparticles, the occupancy would obey

$$f(k) = \frac{\langle E^2(k)\rangle}{2(N_c^2-1)k} = \frac{\langle k^2 A^2(k)\rangle}{2(N_c^2-1)k}\,, \qquad (7)$$

where $2(N_c^2-1)$ just counts degrees of freedom in E and B. One can therefore define f_E and f_B as the occupancy as determined by the electric and magnetic fields by imposing this expression. This is just a way of parameterizing the power spectrum of E and A; but if the degrees of freedom are actually behaving as light quasiparticles, we should observe $f_B \simeq f_E$.

Results for f_E and f_B are shown in fig. 5. The IR contains nonperturbatively large fields which are quasistationary in time. In the UV, the behavior is that of quasiparticles, which become more numerous with time, growing towards a steady state power law spectrum with a spectral index of approximately $f \propto k^{-2}$.

While the IR behavior is quasistationary, it is dynamical, not quasistatic. Chern-Simons number diffuses (not shown), indicating that nonperturbative physics is involved and that there is no long time scale coherence to the soft gauge field configuration.

5 Conclusions

The expansion of the QGP in a heavy-ion collision should lead to a locally anisotropic system. Within the weak-coupling expansion, this implies that plasma instabilities should develop. Plasma instabilities imply a transfer of energy from the "hard" typical excitations to large long-wavelength "soft" non-Abelian magnetic fields. The subsequent evolution of these soft fields requires nonperturbative tools to uncover. In an $\alpha_s \ll 1$ treatment, where the separation between hard and soft scales is parametrically large, we find an intriguing cascade phenomenon. Energy is taken from the hard fields into the soft fields. However, non-Abelian interactions between soft fields keep the would-be unstable fields in a quasisteady state. Instead the energy cascades into classical fields with wave numbers k larger than the unstable field scale, m_∞. The

cascade towards the ultraviolet develops with a power law spectrum $f \propto k^{-\alpha}$ with $\alpha \simeq 2$. This value of the spectral index implies that the cascade particles do not dominate the screening and do not serve as the dominant source of scattering events.

We do not fully understand the implications of these results for thermalization of the QGP even in the case of weak coupling, much less at realistic couplings for current experiments. However, the physics is rich and intriguing and deserves further study.

References

1. PHENIX Collaboration (K. Adcox *et al.*), Nucl. Phys. A **757**, 184 (2005); STAR Collaboration (J. Adams *et al.*), Nucl. Phys. A **757**, 102 (2005); PHOBOS Collaboration (B.B. Back *et al.*), Nucl. Phys. A **757**, 28 (2005); BRAHMS Collaboration (I. Arsene *et al.*), Nucl. Phys. A **757**, 1 (2005).
2. P.F. Kolb, P. Huovinen, U.W. Heinz, H. Heiselberg, Phys. Lett. B **500**, 232 (2001) [hep-ph/0012137]; D. Teaney, J. Lauret, E.V. Shuryak, Phys. Rev. Lett. **86**, 4783 (2001) [nucl-th/0011058]; U.W. Heinz, *Hadron Physics and Relativistic Aspects of Nuclear Physics*, AIP Conf. Proc. **739**, 163 (2004) [nucl-th/0407067].
3. E. Shuryak, Prog. Part. Nucl. Phys. **53**, 273 (2004) [hep-ph/0312227]; M. Gyulassy, L. McLerran, Nucl. Phys. A **750**, 30 (2005) [nucl-th/0405013].
4. D. Molnar, M. Gyulassy, Phys. Rev. C **62**, 054907 (2000) [nucl-th/0005051]; Nucl. Phys. A **697**, 495 (2002) (Nucl. Phys. A **703**, 893 (2002)(E)) [nucl-th/0104073].
5. Z. Xu, C. Greiner, Phys. Rev. C **71**, 064901 (2005) [hep-ph/0406278].
6. P. Aurenche, F. Gelis, H. Zaraket, JHEP **0205**, 043 (2002) [hep-ph/0204146].
7. S. Mrówczyński, M.H. Thoma, Phys. Rev. D **62**, 036011 (2000) [hep-ph/0001164].
8. P. Arnold, G.D. Moore, L.G. Yaffe, JHEP **0301**, 030 (2003) [hep-ph/0209353].
9. E. Braaten, R.D. Pisarski, Nucl. Phys. B **337**, 569 (1990).
10. S. Mrówczyński, A. Rebhan, M. Strickland, Phys. Rev. D **70**, 025004 (2004) [hep-ph/0403256].
11. E.S. Weibel, Phys. Rev. Lett. **2**, 83 (1959).
12. P. Arnold, J. Lenaghan, G.D. Moore, JHEP **0308**, 002 (2003) [hep-ph/0307325].
13. P. Romatschke, M. Strickland, Phys. Rev. D **68**, 036004 (2003) [hep-ph/0304092].
14. J. Ambjorn, T. Askgaard, H. Porter, M.E. Shaposhnikov, Nucl. Phys. B **353**, 346 (1991).
15. D. Bödeker, G.D. Moore, K. Rummukainen, Phys. Rev. D **61**, 056003 (2000) [hep-ph/9907545].
16. A. Rebhan, P. Romatschke, M. Strickland, Phys. Rev. Lett. **94**, 102303 (2005) [hep-ph/0412016]; JHEP **0509**, 041 (2005) [hep-ph/0505261].
17. P. Arnold, G.D. Moore, L.G. Yaffe, Phys. Rev. D **72**, 054003 (2005) [hep-ph/0505212].
18. P. Arnold, G.D. Moore, hep-ph/0509206.